Journal of Constructional Steel Research 71 (2012) 171–181

Contents lists available at SciVerse ScienceDirect

Journal of Constructional Steel Research

Behavior and resistance of beam-column structural elements

Anwar Badawy Badawy Abu-Sena *, Mohamed Salah Al-Din Soliman, Omer Nazmi Ali Abdel-Nabi

Faculty of Engineering (Shobra), Benha University, Egypt

A R T I C L E I N F O

Article history:
Received 27 April 2011
Accepted 12 September 2011
Available online 5 October 2011

Keywords:
Steel beam-column
Lateral torsional buckling
Flexural buckling
Torsional buckling
Finite element non-linear elasto-plastic analysis
Ultimate resistance
Codes of practice

A B S T R A C T

Most of the structural elements in a steel structure are subjected to bending moment and axial force simultaneously. In some elements, one of the two components is relatively small compared to the other. Yet, the smaller component cannot be ignored due to the interactive behavior of the two components. Therefore, it is not adequate to design the beam-column element as a beam or a column by ignoring one of the two load components even if the ignored component is relatively small.

Most of the design codes use empirical interaction equations that are based on semi-experimental semi-analytical results. Most of the design formulae adopted by the design codes do not explicitly account for the geometrical imperfection.

This research aims at investigating the buckling behavior of steel beam-column elements for the sake of developing an analytical model to calculate their ultimate resistance under axial compression and bending moment. The analytical model will be based on Perry-type formulation, and it will account for the effect of initial imperfection. The model will be validated by comparing its results with those obtained by the Finite Element Non-Linear Elasto-Plastic analysis using ANSYS 5.4 program.

Finally, a simple but rational design method based on the model, will be introduced. This method can be applied using a simple mathematical expression or charts and tables. The results of the developed design method will be compared with the design method of the international codes of practice for design of steel structures. On light of these comparisons, design recommendations are introduced.

© 2011 Elsevier Ltd. All rights reserved.

1. Introduction

Resistance and interactive buckling behavior attracted the attention of many researchers over the last four decades, however, due to its importance and complexity, this subject is still receiving the researchers' interest.

In 1977, Kanachalani [14] investigated the in-elastic behavior of 82 steel beam-column. He developed the well-known bilinear interaction equation that is being utilized by many international design codes. The AISC (LRFD) design manual [2] is adopting this bilinear interaction equation. Also, the Egyptian Code of Practice for Steel Design (LRFD) [10] is utilizing this equation.

In 1985, Trahair [15] investigated the accuracy and applicability of the design formulae utilized by the Canadian Standard. He developed a simple computational procedure for estimating the in-plane strength, which generally leads to more accurate prediction than that of the code. He also developed two alternatives for estimating the out-of-plane strength of beam-column.

In 1989, Geng-Shu and Shao-Fan [12] established an interactive buckling theory for built-up beam columns which can be used to determine the ultimate strength of the member taking account of various adverse influences of imperfections (residual stress, member's and chords' initial deflections and load eccentricity). They verified the applicability of the proposed theory by the finite integral method.

In 2004, Aminmansour [3] introduced design aids including charts and tables to facilitate the application of the AISC (LRFD) [2] interaction equation. The proposed approach avoids the application of the iterative technique followed to select the most appropriate steel section. Several design examples have been given to explain the application of the proposed design approach.

In 2004, Gonçalves and Camotim [13], examined the beam-column design approach adopted by the Eurocode (EC3) [11], using the finite element non-linear analysis utilizing ABAQUS program. They compared the code design approach to the finite element analysis for different loading and boundary conditions. They highlighted the sensitivity of the code estimated strength to the C_m value compared to the FE analysis. They concluded that the EC3 strength estimate is excellent for the in-plane strength of members with arbitrary boundary conditions. For low axial force, they concluded that the EC3 strength estimate is quite conservative.

This research aims at investigating the interactive buckling behavior in beam-column. Two types of interaction will be studied; the elastic linear interaction and the non-linear interaction. The first type affects the critical buckling modes and the critical buckling loads. The second type affects the beam-column resistance. Mathematical models will be developed to predict both the interactive buckling stress and the

* Corresponding author. Tel.: +20 2 011 067 6655.
E-mail address: abbadawy@yahoo.com (A.B. Badawy Abu-Sena).

0143-974X/$ – see front matter © 2011 Elsevier Ltd. All rights reserved.
doi:10.1016/j.jcsr.2011.09.012

ultimate resistance. Finite Element analysis using ANSYS program will be applied to validate the results obtained from the mathematical models. Eigen value analysis will be used to verify the critical buckling interaction mathematical model, and non-linear elasto-plastic analysis will be utilized to validate the resistance estimation model. Finally, the developed models will be used to establish a rational simple design method that can be used to predict the ultimate resistance of beam-column structural elements.

2. Critical buckling interaction

In general, the critical buckling load does not represent the strength of members. In beam column members, the ultimate resistance is always below the critical buckling loads. However, investigating the critical buckling interaction still has its importance, because the critical buckling loads will be required in estimating the member strength.

In a column of doubly symmetric cross section, there are three individual buckling modes, flexural buckling about minor axis, torsional buckling and flexural buckling about the major axis. In singly symmetric section, one of the two flexural modes interacts with the torsional mode producing the torsional-flexural mode reducing the number of individual modes to only two [1,8,16]. In beams there is only one overall buckling mode; that is the lateral torsional buckling mode [5].

In the presence of axial load and bending moment, i.e., in a beam-column element, the lateral torsional buckling mode under bending moment initiates all the overall buckling modes of column, resulting in a single buckling mode that has three degrees of freedom v(x), w(x) and θ(x) as indicated in Fig. 1. The interactive buckling load of the final mode is given by Trahair et al. [16]. The interactive critical buckling loads are related by the following expression:

$$\left(\frac{M_{cr}}{M_{LTz}}\right)^2 = \left(1-\frac{P_{cr}}{P_{Ez}}\right)\left(1-\frac{P_{cr}}{P_{Ey}}\right)\left(1-\frac{P_{cr}}{P_T}\right) \tag{1}$$

Where;

M_{cr} and P_{cr} are the critical buckling moment and axial force respectively
M_{LTz} is the lateral torsional buckling moment about Z-axis (minor axis)
P_{Ez}, P_{Ey} are the critical buckling loads of the two individual Euler modes about Z and Y axes respectively
P_T is the torsional buckling critical load.

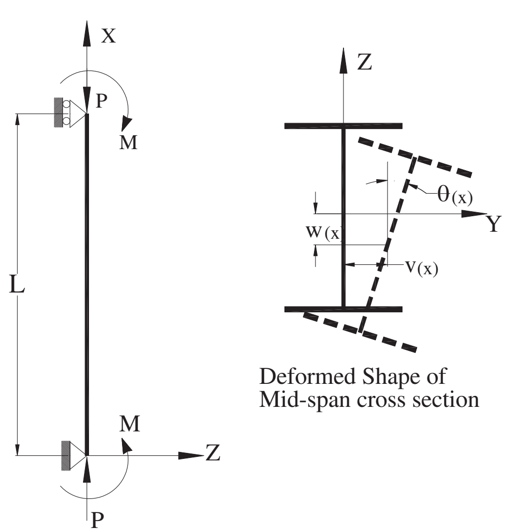

Fig. 1. Beam-column boundary conditions, loads, axes and deformed shape.

Critical loads of the individual buckling modes are given by the following expressions [16]:

$$M_{LTz} = \frac{\pi}{L}\sqrt{\frac{EI_z\left(GJ+\frac{\pi^2 EC_w}{L^2}\right)}{\gamma}} \tag{2.a}$$

$$P_{Ez} = \frac{\pi^2 EI_z}{(KL_z)^2} \tag{2.b}$$

$$P_{Ey} = \frac{\pi^2 EI_y}{\left(KL_y\right)^2} \tag{2.c}$$

$$P_T = \frac{1}{r_o^2}\left(GJ+\frac{\pi^2 EC_w}{L^2}\right) \tag{2.d}$$

As per Ref. [16], the relation between the lateral displacement (v(x)), and section rotation (θ(x)) is given by:

$$v(x) = \frac{M_{cr}}{P_{Ez}-P_{cr}}\theta(x) \tag{3}$$

Where E is the modulus of elasticity, I_z and I_y are the minor and major moments of inertia as shown in Fig. 1, G is the shear modulus, J is the St. Venant torsional constant, C_w is the warping constant, L is the beam length and γ is a geometrical factor; that equals $(1-I_z/I_y)$.

For the sake of comparison and better understanding of the critical buckling interaction in beam-column Finite Element analysis has been performed using ANSYS program [4], for two beams of different geometries. The first beam is an I-section; that has the following dimensions: b_f=200 mm, t_f=16 mm, d_w=600 mm and t_w=8 mm. The second beam has also an I-section; that has the following dimensions: b_f=150 mm, t_f=12 mm, d_w=500 mm and t_w=10 mm. Dimensions of the two beams are selected to avoid local and distortional buckling

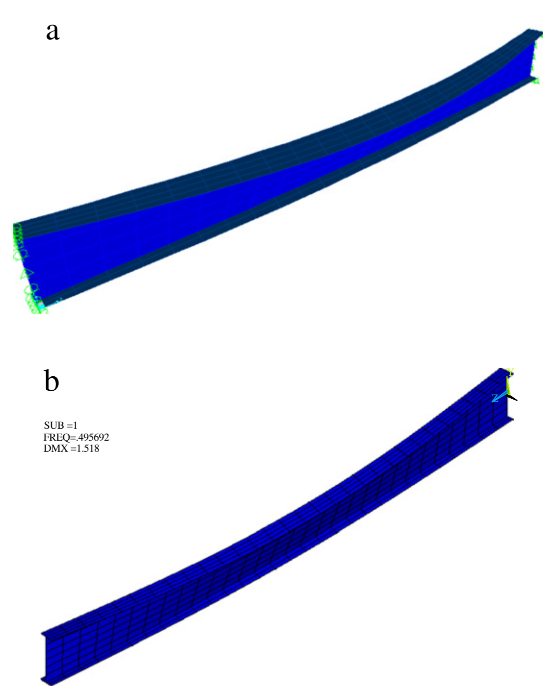

Fig. 2. (a) Buckled shape for first section, L=6.0 m, $\frac{P_{cr}}{P_{Ez}}=0.346$, $\frac{M_{cr}}{M_{LTz}}=0.736$. (b) Buckled shape for second section, L=6.0 m, $\frac{P_{cr}}{P_{Ez}}=0.646$, $\frac{M_{cr}}{M_{LTz}}=0.535$.

completely. In the vast majority of the studied cases, the interactive buckling mode was the first Eigen mode. Twenty nine bending moment–normal force combinations have been considered for the first section and twenty three combinations have been considered for the second section. The considered cases include; pure axial compression, pure bending moment, combined bending and compression and combined bending and tension force. Sample of the buckled deformed shapes of the two beams are shown in Fig. 2a and b respectively.

Fig. 3a and b shows a comparison between the results obtained from the finite element analysis and the interactive critical buckling stress predicted by Eq. (1).

It can be easily concluded from Fig. 3a and b that, there is an excellent agreement between the critical buckling interaction predicted by the analytical solution expressed by Eq. (1) and that shown by the finite element analysis.

3. Non-linear interaction

Young's equation for imperfect columns was employed by Perry to develop a mathematical model for calculating the ultimate resistance of columns undergoing flexural buckling. This model is adopted by the British Standards BS5950 [7] and the Euro Code EC3 [11]. The same concept was applied by references [6] and [9] to estimate buckling resistance of beams undergoing lateral torsional buckling in presence of initial imperfection.

Applying the Perry formulation enables the designer to take the effect of initial imperfection into account. Most of the design codes neglect the effect of initial imperfection value, although it may have a significant effect on the element resistance as will be illustrated in this research.

To investigate the non-linear interaction of a beam-column structural element in presence of initial imperfection, a mathematical model will be developed to account for the geometrical and material non-linearity. The model will be verified by comparison to the finite element non-linear elasto-plastic analysis results. The proposed model is based on Perry-type formulation that is based on Young's equation of imperfect column. A rational design method based on the developed analytical model will be introduced and its results will be compared with those of the design codes of practice.

3.1. Mathematical formulation

For a simply supported beam-column with ends prevented from twisting and free to warp, the angle of rotation, and accordingly

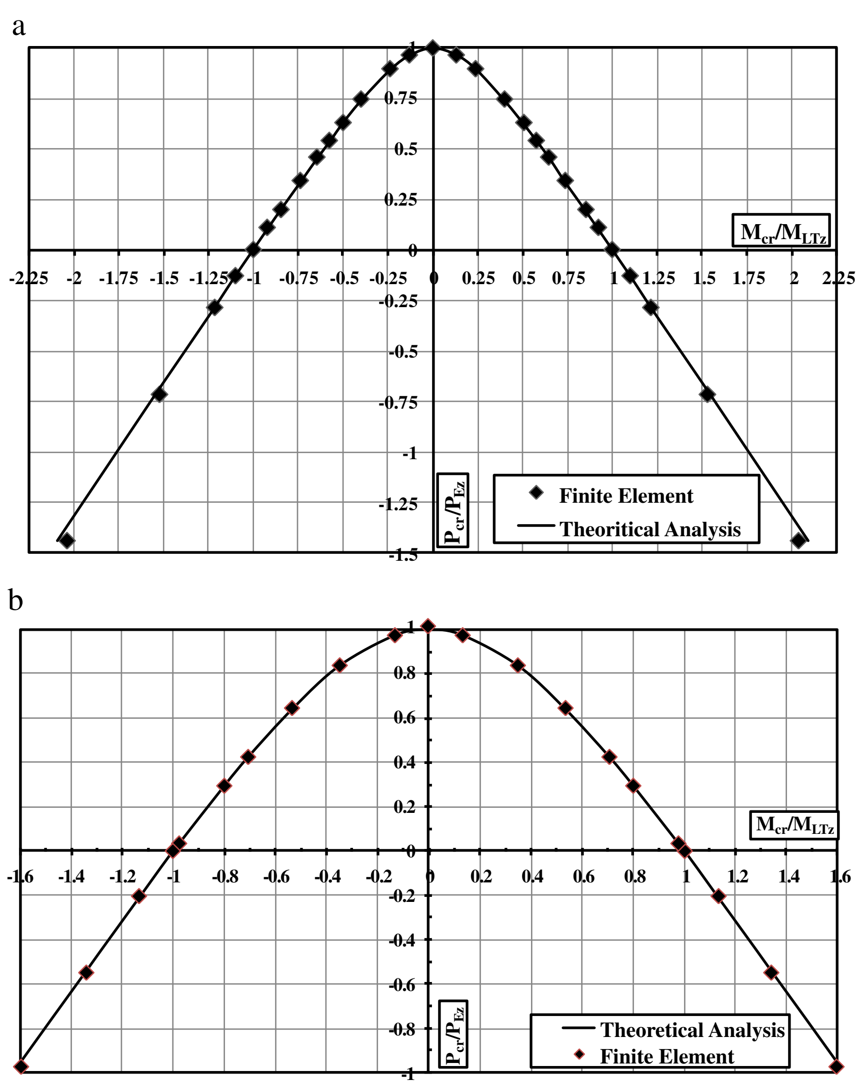

Fig. 3. (a) Comparison between FE and theoretical solution for critical buckling interaction for first section; $b_f = 200$ mm, $t_f = 16$ mm, $d_w = 600$ mm, $t_w = 8$ mm, and $L = 6.0$ m. (b) Comparison between FE and theoretical solution for critical buckling interaction for second section; $b_f = 150$ mm, $t_f = 12$ mm, $d_w = 500$ mm, $t_w = 10$ and $L = 6.0$ m.

the lateral displacement, varies sinusoidally along the beam length. Fig. 1 shows the deformed shape of the mid-span cross section. For an initial imperfection affine to the Eigen mode, the initial rotation and lateral displacement can be expressed by the following equations.

$$\theta_o(x) = \theta_o \sin\left(\frac{\pi x}{L}\right) \tag{4.a}$$

$$v_o(x) = v_o \sin\left(\frac{\pi x}{L}\right) \tag{4.b}$$

Where θ_o and v_o are the initial imperfection amplitudes at mid-span. The relation between θ_o and v_o at mid-span is given by Eq. (3).

Young's equation gives the relation between the applied load and the lateral deformation for a column undergoing flexural buckling. For beams undergoing lateral torsional buckling Young's equation has been successively applied by [6,9] to predict the ultimate resistance of the beams. However, this type of formulation can be applied on beam-column with replacing the critical buckling loads of the individual modes by the interactive buckling loads obtained from Eq. (1). According to Young's equation, the relation between deformation at any load level and the initial deformation is given by:

$$\theta = \frac{\theta_o}{1-M/M_{cr}} \tag{5.a}$$

$$v = \frac{v_o}{1-M/M_{cr}} \tag{5.b}$$

Where, θ and v are the rotation and lateral displacement at any applied load (M and P), and M_{cr} is the interactive critical buckling moment as per Eq. (1). The relation between θ/v and the applied moment is shown in Fig. 4.

The additional deformations (θ_1 and v_1) produce additional bending and warping stress, these deformations are given by the following expression:

$$\theta_1 = \theta - \theta_o = \frac{M}{M_{cr}-M}\theta_o \tag{6.a}$$

$$v_1 = v - v_o = \frac{M}{M_{cr}-M} v_o \tag{6.b}$$

The additional rotation (θ_1) produces an additional warping stress, while the additional lateral displacement (v_1) produces an additional

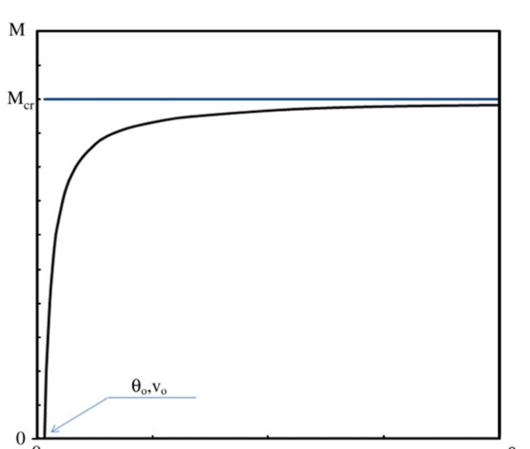

Fig. 4. Load–displacement relationship (Young's equation).

moment about the minor axis (M_{zm}), which in turn produces an additional normal stress. The additional M_{zm} can be given by the following expression:

$$M_{zm}(x) = -EI_z \frac{d^2 v_1(x)}{dx^2} = EI_z\left(\frac{M}{M_{cr}-M}\right) v_o \frac{\pi^2}{L^2} \sin\frac{\pi x}{L} \tag{7.a}$$

At mid-span M_{zm} has a maximum value that is given by the following expression:

$$M_{zm} = EI_z\left(\frac{M}{M_{cr}-M}\right) v_o \frac{\pi^2}{L^2} \tag{7.b}$$

Due to the translation of the cross section, the applied axial force produces additional moments about the two principal axes of the cross section. The values of these additional bending moments are given by the following expression:

$$M_{zp}(x) = P * v(x) = P\left(\frac{M_{cr}}{M_{cr}-M}\right) v_o \sin\frac{\pi x}{L} \tag{8.a}$$

$$M_{yp}(x) = P * w(x) = P\left(\frac{M_{cr}}{M_{cr}-M}\right) w_o \sin\frac{\pi x}{L} \tag{8.b}$$

As will be illustrated later, considering the additional moment about the major axis (M_{yp}) will result in complicating the final solution because it results in a third order equation. On the other hand ignoring this moment relatively simplifies the final expression. It has been noticed that the effect of this component is minor and its contribution to the final ultimate load is less than 1%. That is due to two reasons, the first is the relatively small value of w_o compared to v_o, and the second is the fact that this moment is about the major axis, and accordingly it will be divided by the major section modulus resulting in a very small stress component. Therefore, it was decided to omit this component from the final expression of the ultimate resistance.

The additional rotation (θ_1) produces an additional normal warping stress. This stress has maximum values at the outside of flanges. For the rotation of Fig. 1, the left side of the top flange and the right side of the bottom flange will have compressive stress. The other two corners will have tensile stress as shown in Fig. 5. The maximum value of the warping stress at mid-span is given by the following expression [6]:

$$\sigma_w = \frac{\pi^2 E}{L^2}\theta_1 \frac{d_w}{2}\frac{b_f}{2} = \frac{\pi^2 E}{L^2}\frac{d_w * b_f}{4}\left(\frac{M}{M_{cr}-M}\right)\theta_o \tag{9}$$

Where; d_w and b_f are the beam depth and width respectively.

The additional bending moment given by Eqs. (8.a) and (8.b), will produce additional axial stresses that are given by the following expressions:

$$\sigma_{zm} = \frac{M_{zm}}{Z_z} \tag{10.a}$$

$$\sigma_{zp} = \frac{M_{zp}}{Z_z} \tag{10.b}$$

The additional stresses given by Eqs. (9), (10.a) and (10.b) should be added to the stress produced by the applied loads (P and M). This will increase the stress at some corners and reduce it at the others around the section. Fig. 5 shows the stress distribution due to the applied loads and due to the additional straining actions. For initial imperfection affine to the deformed shape shown in Fig. 1, all stress components at the left corner of the upper flange will be compressive, accordingly failure will take place first at this corner.

In this research the *first yield criteria* will be adopted as a failure criterion. This concept has been applied by many researchers, e.g.,

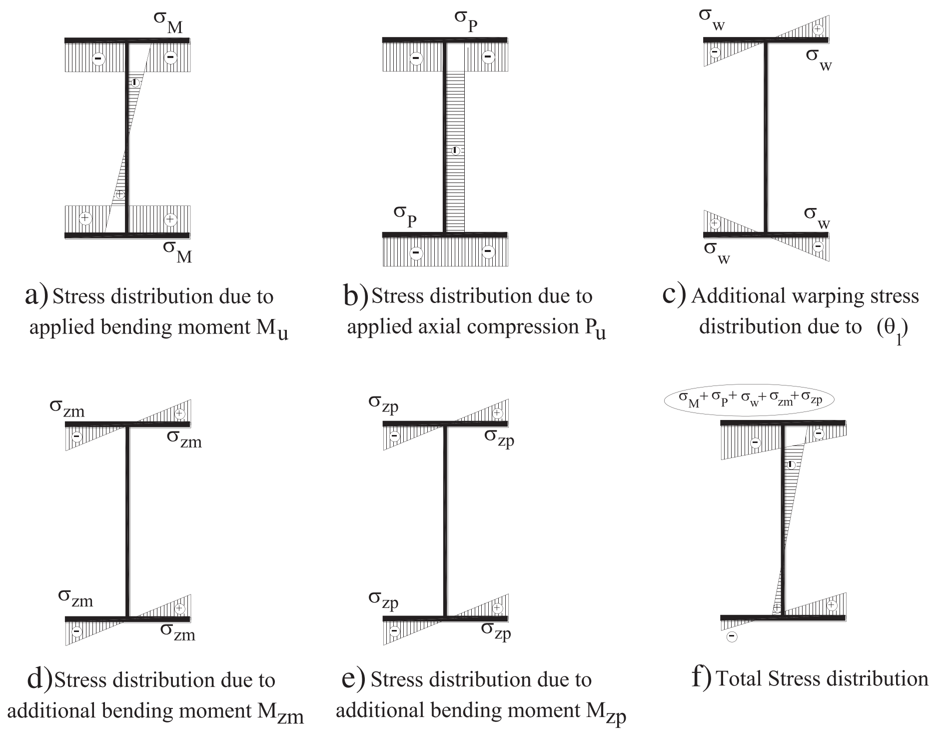

Fig. 5. Stress distribution due to applied and additional straining actions.

references [6,9]. According to this concept, the ultimate resistance is represented by the load that causes first yield around the cross section. That means, the ultimate loads (P_u and M_u) are those loads that cause the first yield to take place at the point of maximum stress. From Fig. 5, the total stress at the left-hand-side corner of the top flange should be equated to the material yield stress to obtain the ultimate resistance. Applying this concept leads to the following expression:

$$\sigma_y = \sigma_M + \sigma_P + \sigma_w + \sigma_{zm} + \sigma_{zp} \tag{11}$$

From Eq. (11), the following expression can be developed;

$$\frac{M_u}{Z_y} + \frac{P_u}{A} + \frac{\pi^2 E}{L^2}\ \frac{d_w{}^* b_f}{4}\left(\frac{M_u}{M_{cr}-M_u}\right)\theta_o + \\ + \frac{EI_z}{Z_z}\left(\frac{M_u}{M_{cr}-M_u}\right)v_o\frac{\pi^2}{L^2} + \frac{P_u}{Z_z}\left(\frac{M_{cr}}{M_{cr}-M_u}\right)v_o = \sigma_y \tag{12}$$

Where, Z_y and Z_z are the modulii of section about the major and minor axes respectively. For an eccentricity (e), P_u can be replaced by M_u/e. Multiplying both sides of Eq. (12) by Z_y, and rearranging the terms of the equation, result at the following expression:

$$\mu^* M_u^2 - (M_o + (\mu + \eta^* v_o)M_{cr})M_u + M_o{}^* M_{cr} = 0 \tag{13}$$

Where: μ and η are geometrical parameters given by:

$$\mu = 1 + \frac{Z_y}{A^* e} \tag{14.a}$$

$$\eta = \frac{Z_y}{e^* Z_Z} + \frac{P_{Ez}{}^* Z_y}{M_{cr}{}^* Z_z} + \frac{b_f{}^* P_{Ey}(P_{Ez}-P_{cr})}{2M_{cr}^2} \tag{14.b}$$

v_o is the initial lateral imperfection amplitude at mid-span, M_u is the ultimate moment capacity of the beam-column element, M_o is the yield moment about major axis $= Z_y{}^*\sigma_y$, and M_{cr} is the interactive critical buckling moment obtained from Eq. (1). Obtaining M_u from Eq. (13) for a certain eccentricity, then P_u can be calculated. The ultimate bending moment can be obtained from Eq. (13), according to which the ultimate bending moment can be given by:

$$M_u = \frac{1}{2\mu}\left(M_o + (\mu + \eta^* v_o)M_{cr} \mp \sqrt{(M_o + (\mu + \eta^* v_o)M_{cr})^2 - 4\mu M_o{}^* M_{cr}}\right) \tag{15}$$

$$P_u = \frac{M_u}{e} \tag{16}$$

If the additional moment about the major axis (M_{yp}) given by Eq. (8.b) was considered in the mathematical formulation was going to be more complicated, and Eq. (13) was going to be a third order equation. As clarified earlier the effect of this term to the final ultimate resistance was found to be minor.

3.2. Finite element non-linear analysis

ANSYS Finite Element Program [4] is used as a numerical tool to verify the model developed in this research. Analyses have been carried out for the second section, for different level of initial imperfections. Four-noded thick shell element is used in all the FE analyses in this research. The number of elements in the flanges is 4, and 6 elements are used for the web. The number of elements along the beam length is 30, as shown in Fig. 2b. The boundary conditions are chosen to verify the simply supported conditions, i.e., the beam ends are prevented from translation in Y and Z-directions and rotation about the X-axis. Warping and rotation about Y and Z axes at the beam ends are allowed. The initial imperfections for all the studied cases were chosen to be affine to the first Eigen mode (interactive mode between lateral torsional and flexural modes). Different eccentricities (e) were studied from zero (pure axial force) to infinity (pure bending). Two different values of initial imperfections have been considered $v_o = L/1000$ and $v_o = L/2000$.

Fig. 6a shows the deformed shape obtained from the finite element non-linear elasto-plastic analysis for the second section, with L = 6 m for initial imperfection $v_o = L/2000$. This figure illustrates the deformed shape at first yield and during the post-buckling

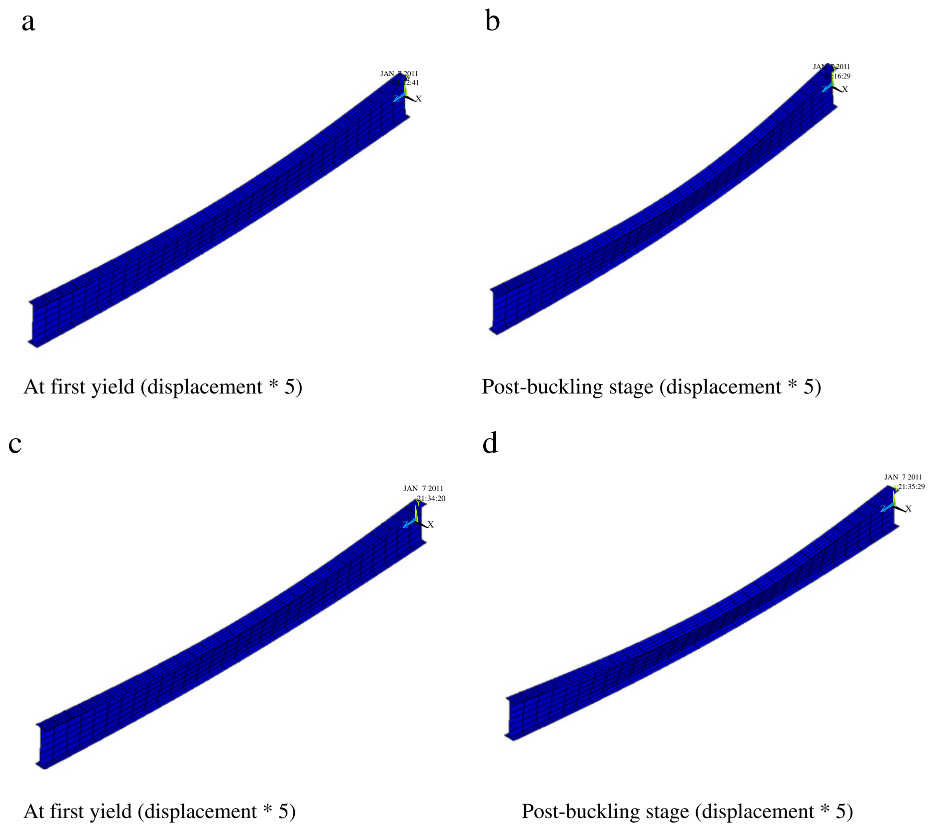

Fig. 6. (a) Deformed shape of the second section, $L = 6$ m, $v_o = L/2000 = 3$ mm, $e/d_w = 0.5$. (b) Deformed shape of the second section, $L = 6$ m, $v_o = L/1000 = 6$ mm, $e/d_w = 0.5$.

stage. Fig. 6b shows the deformed shape of the same beam, with $v_o = L/1000$.

In the next section, results of the analytical model developed in this section will be compared with those obtained by the finite element non-linear elasto-plastic analysis. To verify the developed model, ultimate resistance, load–displacement curves and stress distribution at first yield around the cross section obtained by the model will be compared to the corresponding results obtained from ANSYS.

4. Results and comparisons

Eqs. (15) and (16) have been applied to obtain the ultimate resistance for beam columns of I-sections. The equations have been applied for different values of initial imperfections, that are $v_o = 0$, L/2000, L/1000, and L/500, the corresponding value of θ_o was estimated from Eq. (3). Different eccentricities ranging from zero (axially loaded columns) to infinity (pure bending) were investigated. Sixteen finite elements non-linear elasto-plastic analysis were performed for $v_o = L/2000$ and L/1000, and with $e/d_w = 0$, 0.08, 0.25, 0.5, 1.0, 1.67, 16.7, and infinity.

Fig. 7a and b shows comparisons between the bending moment-displacement and axial force–displacement curves obtained from Eq. (5.b) and those obtained from the finite element non-linear analysis for initial imperfection of L/2000 and $e/d_w = 0.5$. Fig. 8a and b shows the same comparison for an initial imperfection of L/1000 and for the same value of eccentricity.

Fig. 9 shows a comparison between the interaction diagram obtained from the developed model (Eqs. (15) and (16)), and the results obtained from the finite element analysis for different values of initial imperfections.

Fig. 10a shows a comparison between the stress distribution around the cross section obtained from the mathematical model and those obtained from the finite element analysis at first yielding for initial imperfection $v_o = L/2000$ and eccentricity $e/d_w = 0.5$.

Fig. 10b shows a similar comparison between the mathematical model and the finite element non-linear elasto-plastic analysis at first yield for initial imperfection $v_o = L/1000$ and eccentricity $e/d_w = 0.5$.

The stress distribution obtained by the analytical model is based on Eqs. (9) to (11) that are illustrated in Fig. 5.

It can be noticed from Figs. 7 and 8, that the lateral displacement–load relationship is well predicted by the developed model compared to the same relations obtained from the finite element analysis. Load–displacement relations obtained from both solutions are almost coincident until the first yield or ultimate load point, where the theoretical relation continues approaching the critical buckling load and the numerical relation starts the unloading stage. This conclusion is applicable to all studied cases.

From Fig. 9, it is clear that the strength and interaction curve predicted by the developed analytical model agree well with the interactive strength obtained from the finite element non-linear analysis for all the investigated eccentricities and initial imperfections. It can be also noticed that, the magnitude of initial imperfection has a minor effect to the interactive curve (relation between M_u/M_{uo} and P_u/P_{uo}). However, that does not mean that the initial imperfection is of insignificant effect, because it is still affecting the values of M_{uo} and P_{uo} themselves. For example, for $e/d_w = 0.5$, for initial imperfections of 0, L/2000, L/1000, L/500, the ultimate load ratios are $M_u/M_{uo} = 0.534$, 0.528, 0.522 and 0.512 and $P_u/P_{uo} = 0.647$, 0.626, 0.616 and 0.606 respectively. As mentioned, the initial imperfection values still have significant effect on the ultimate loads M_{uo} and P_{uo}, where for the same level of imperfections, $M_u = 144$, 125, 112 and 94 kN m and $P_u = 391$, 346, 312 and 262 kN respectively.

From Fig. 10a and b, it can be noticed that the stress distribution around the beam cross section predicted by the developed analytical model is in a good agreement with the distribution obtained by the

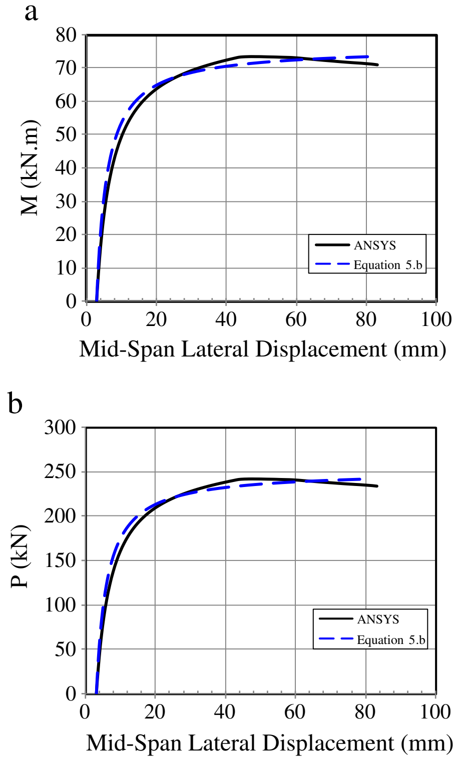

Fig. 7. (a) Moment–displacement curves for $v_o = L/2000$, $e/d_w = 0.5$. (b) Force–displacement curves for $v_o = L/2000$, $e/d_w = 0.5$.

finite element analysis. For all studied cases, the predicted points of first yield at the two methods of analyses are the same.

Therefore it could be deduced that, the developed model predicts accurately the interactive ultimate resistance, the force/moment–displacement relationship and the stress distribution around the cross section compared to the finite element non-linear elasto-plastic analysis. The analytical model takes account of the effect of initial imperfection. Therefore this model can be used as a rational simple design method for estimating the ultimate resistance of beam-column structural elements. Results of the developed design method will be compared to the design rules adopted by the different codes of practice in next section.

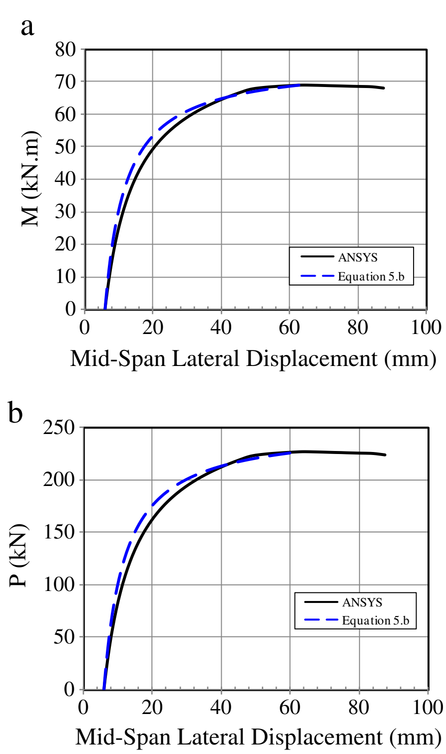

Fig. 8. (a) Moment–displacement curve for $v_o = L/1000$, $e/d_w = 0.5$. (b) Force–displacement curves for $v_o = L/1000$, $e/d_w = 0.5$.

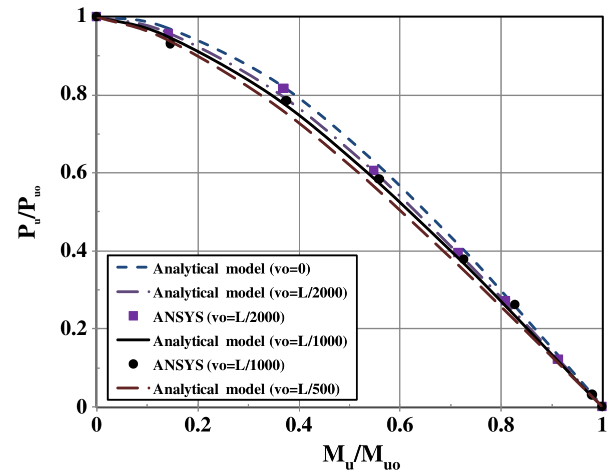

Fig. 9. Comparison between the interaction diagram obtained from the developed model and finite element non-linear analysis ($b_f = 150$ mm, $t_f = 12$ mm, $d_w = 500$ mm, $t_w = 10$ and $L = 6.0$ m), M_{uo} = Pure bending ultimate capacity (beam), P_{uo} = Pure axial ultimate capacity (column).

5. Proposed design method and design codes

5.1. AISC (LRFD), 2005 and ECP (LRFD), 2008

The Egyptian Code of Practice (ECP) (LRFD), 2008 [10] adopted the same concept and even the same interactive equations used by the AISC (LRFD), 2005 [2]. The two codes adopted a bilinear interaction equation to represent the relation between ultimate moment and normal force. According to the two codes, the interaction equation is given by the following expression:

$$\frac{P_u}{\phi P_n} + \frac{8}{9}\left(\frac{M_{uy}}{\phi_b M_{ny}} + \frac{M_{uz}}{\phi_b M_{nz}}\right) \le 1.0 \quad \text{for} \quad \frac{P_u}{\phi P_n} \ge 0.2 \tag{17.a}$$

$$\frac{P_u}{2\phi P_n} + \left(\frac{M_{uy}}{\phi_b M_{ny}} + \frac{M_{uz}}{\phi_b M_{nz}}\right) \le 1.0 \quad \text{for} \quad \frac{P_u}{\phi P_n} < 0.2 \tag{17.b}$$

Where, P_u, M_{uy} and M_{uz} are the ultimate axial force and bending moments about the two principal axes, P_n, M_{ny} and M_{nz} are the nominal capacities (including flexural and lateral torsional buckling effect) of the element in pure axial compression and pure bending respectively, and ϕ and ϕ_b are the resistance factors for axial compression and pure bending. AISC and ECP adopts a value of 0.9 for ϕ_b, while for ϕ the LRFD uses a value of 0.9, and the ECP uses a value of 0.85.

5.2. BS5950, 2002

The British Standard BS5950, 2002 [7] adopts many interactive formulae for the design of beam-column structural elements. The

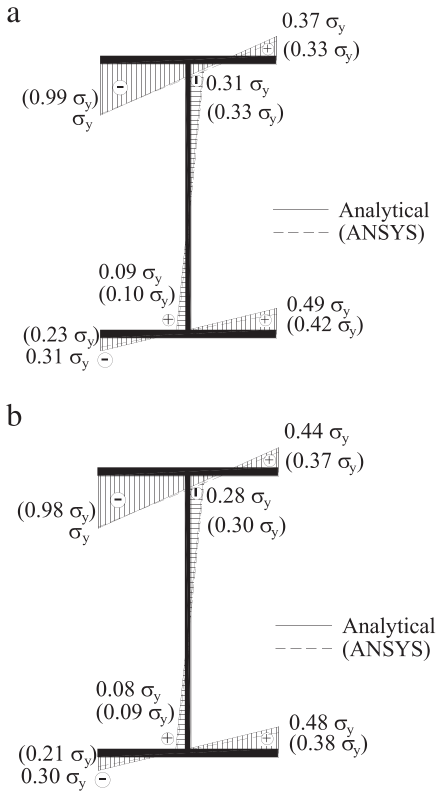

Fig. 10. (a) Comparison between stress distribution obtained by analytical solution and finite element analysis ($v_o = L/2000$, $e/d_w = 0.5$), $P_u/P_{uo} = 0.63$, $M_u/M_{uo} = 0.53$. (b) Comparison between stress distribution obtained by analytical solution and finite element analysis ($v_o = L/1000$, $e/d_w = 0.5$), $P_u/P_{uo} = 0.61$, $M_u/M_{uo} = 0.52$.

first formula is to check the cross section capacity. For a compact section, this formula is given below:

$$\frac{P_u}{P_y} + \frac{M_{uy}}{M_{cy}} + \frac{M_{uz}}{M_{cz}} \le 1.0 \tag{18.a}$$

The other formulae are to check the buckling capacity in and out of plane. A simplified general method and a more-exact method for I and H sections to verify the section buckling capacity. According to the more-exact method, the following verifications should be performed:

$$\frac{P_u}{P_{cy}} + \frac{m_y M_{uy}}{M_{cy}}\left(1 + 0.5\frac{P_u}{P_{cy}}\right) + 0.5\frac{m_{zy} M_{uz}}{M_{cz}} \le 1.0 \text{ (For major axis (Y) buckling axis)} \tag{18.b}$$

$$\frac{P_u}{P_{cz}} + \frac{m_{LT} M_{LT}}{M_b} + \frac{m_z M_{uz}}{M_{cz}}\left(1 + \frac{P_u}{P_{cz}}\right) \le 1.0 \text{ (For lateral torsional buckling)} \tag{18.c}$$

$$\frac{m_y M_{uy}}{M_{cy}} \frac{\left(1 + 0.5\frac{P_u}{P_{cy}}\right)}{\left(1 - \frac{P_u}{P_{cy}}\right)} + \frac{m_z M_{uz}}{M_{cz}} \frac{\left(1 + \frac{P_u}{P_{cz}}\right)}{\left(1 - \frac{P_u}{P_{cz}}\right)} \le 1.0 \text{ (For interactive buckling)} \tag{18.d}$$

Where; m_y, m_z, m_{zy}, m_{LT} are the bending moment shape factors that equal 1.0 for uniform bending moment, P_y, P_{cy} and P_{cz} are the squash axial load, and buckling capacities about Y and Z axes respectively, and M_b, M_{cy} and M_{cz} are the lateral torsional buckling moment and bending capacities about Y and Z axes respectively. In our case, for the sake of comparison, Eq. (18.c) that covers the interaction between lateral torsional and minor axis flexural buckling will be applied.

5.3. Euro Code EC3 1996

The Euro Code E3, 1996 [11], adopts three criteria to estimate the design strength of beam columns. The first criterion is the cross section strength, that is covered in Section 5.4.8, and concerned with the cross section shape, manufacturing, and the presence of bolts hall. For an I-section, this criterion does not govern the beam-column design. The other two criteria cover the beam-column bending and buckling strength. According to Section 5.5.4 of the EC3 code, for class 1 and 2 sections (not slender in local buckling), the following two criteria must be satisfied

$$\frac{N_{Sd}}{\chi_{\min} A f_y/\gamma_{M1}} + \frac{K_y M_{y.Sd}}{W_{pl.y} f_y/\gamma_{M1}} + \frac{K_z M_{z.Sd}}{W_{pl.z} f_y/\gamma_{M1}} \le 1.0 \tag{19.a}$$

$$\frac{N_{Sd}}{\chi_z A f_y/\gamma_{M1}} + \frac{K_{LT} M_{y.Sd}}{\chi_{LT} W_{pl.y} f_y/\gamma_{M1}} + \frac{K_z M_{z.Sd}}{W_{pl.z} f_y/\gamma_{M1}} \le 1.0 \tag{19.b}$$

Where; N_{Sd}, $M_{y.Sd}$, $M_{z.Sd}$ are the ultimate straining actions on the structural elements, χ_{min} is the smaller value of χ_y and χ_z. χ_y and χ_z are buckling reduction factors about Y and Z axes respectively, these factors are given below. γ_{M1} represents the resistance factor, f_y is the material yield stress, A is the cross section area, $W_{pl.y}$, $W_{pl.z}$ are the plastic modulii of section about Y and Z axes respectively. K_y, K_z and K_{LT} are parameters given by Eqs. (21.a),(21.b).

$$\chi_{y,z,LT} = \frac{1}{\phi_{y,z,LT} + \sqrt{\phi^2_{y,z,LT} - \bar{\lambda}^2_{y,z,LT}}} \le 1.0 \tag{20.a}$$

$$\phi_{y,z,LT} = 0.5\left(1 + \alpha_{y,z,LT}\left(\bar{\lambda}_{y,z,LT} - 0.2\right) + \bar{\lambda}^2_{y,z,LT}\right) \tag{20.b}$$

$$\bar{\lambda}_{y,z} = \sqrt{\frac{\beta_A A f_y}{N_{cr(y,z)}}} \tag{20.c}$$

$$\bar{\lambda}_{LT} = \sqrt{\frac{\beta_w W_{ply} f_y}{M_{cr}}} \tag{20.d}$$

β_A and β_w are section parameters, equal 1.0 for section of class 1 and 2. α_y, α_z and α_{LT} are imperfection parameters, given by; $\alpha_y = 0.21$, $\alpha_z = 0.34$ and $\alpha_{LT} = 0.21$.

$$K_{y,z} = 1 - \frac{\mu_{y,z} N_{Sd}}{\chi_{y,z} A f_y} \le 1.5 \tag{21.a}$$

$$K_{LT} = 1 - \frac{\mu_{LT} N_{Sd}}{\chi_z A f_y} \le 1.0 \tag{21.b}$$

$$\mu_{y,z} = \bar{\lambda}_{y,z}\left(2\beta_{My,z} - 4.0\right) + \left(\frac{W_{pl.y,z} - W_{el.y,z}}{W_{el.y,z}}\right) \le 0.9 \tag{21.c}$$

$$\mu_{LT} = 0.15\bar{\lambda}_z \beta_{M.LT} - 0.15 \le 0.9 \tag{21.d}$$

β is an equivalent uniform moment factor for flexural buckling as per Fig. 5.5.3 of the EC3.

Figs. 11 and 12 show comparisons between the proposed design method and the design methods adopted by the international codes of practice for two different sections and spans. The first section (Fig. 11) has; $b_f = 200$ mm, $t_f = 16$ mm, $d_w = 600$ mm, $t_w = 8$ mm, with lengths L = 4.0 m, 8.0 m, 12.0 m and 16.0 m. The second section (Fig. 12) has $b_f = 150$ mm, $t_f = 12$ mm, $d_w = 500$ mm, $t_w = 10$ with lengths L = 3.0 m, 6.0 m, 9.0 m and 12.0 m.

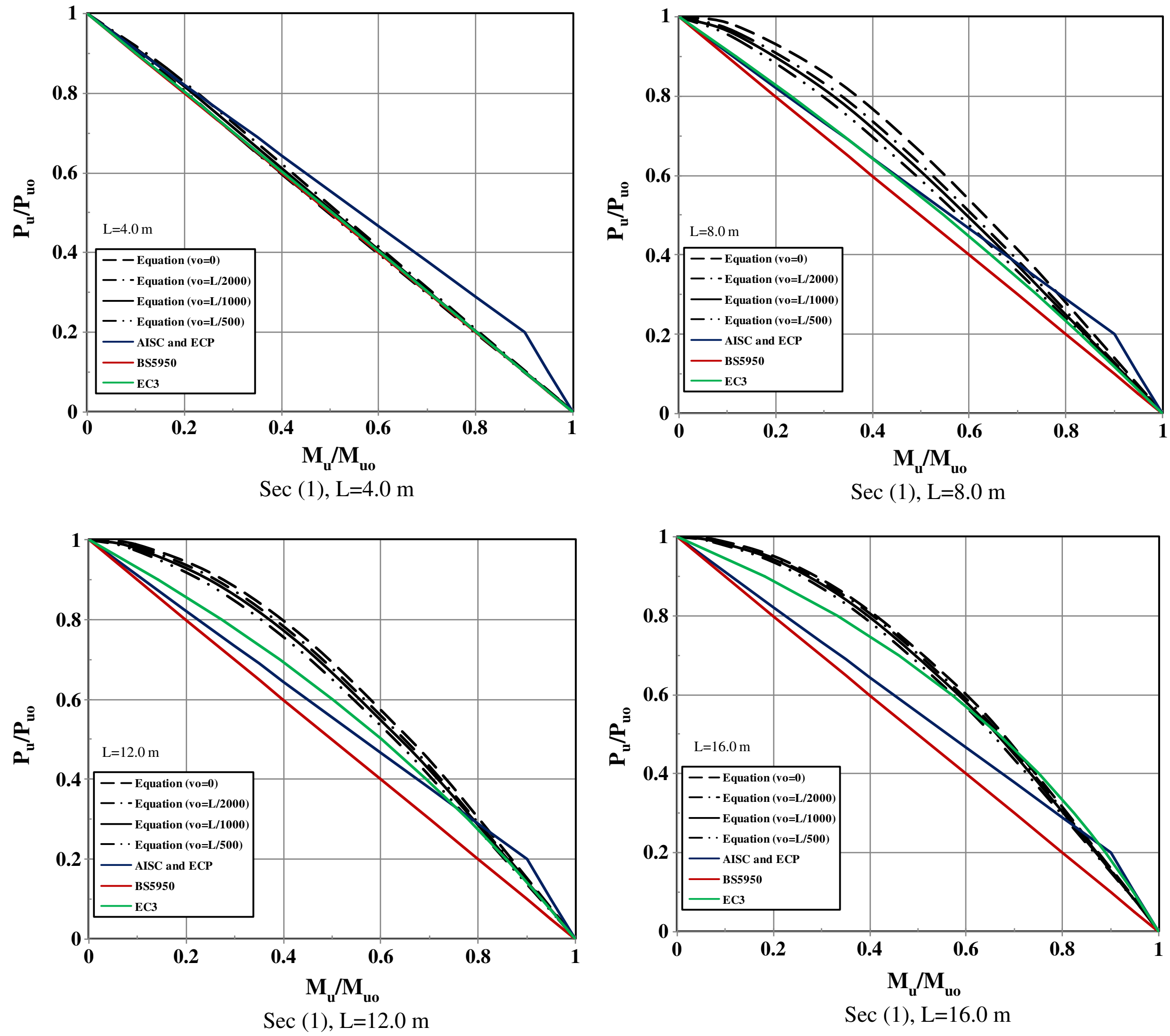

Fig. 11. Comparison between the proposed design method and the design codes methods for the first I-section, $b_f = 200$ mm, $t_f = 16$ mm, $d_w = 600$ mm, $t_w = 8$ mm, L = 4, 8, 12 and 16 m.

From Figs. 11 and 12, it can be concluded that the curvature of the proposed interaction curve is not constant, i.e., for short columns the interaction curve is almost straight line that is very close to the British standard equation, and for long columns the curvature increases and the deviation from the British standard increases as well. The BS5950 interaction curve is always conservative compared to the analytical method. However, the difference between the BS5950 equation and the proposed design method is minimal for short columns, and it increases with increasing the column length. For a column having the first cross section, and column height of 4.0 m, the result obtained by the BS5950 are almost coincidence with those of the proposed method.

The bi-linear interaction approach adopted by the AISC and ECP are non-conservative for short column length, as can be concluded from Fig. 11 for L = 4.0 m and Fig. 12 for L = 3.0 m. Even for longer spans, the AISC/ECP results are also non-conservative compared to the analytical method, for lower axial force ($P_u/P_{uo} < 0.3$). The AISC/ECP design method is conservative for relatively higher axial load ($P_u/P_{uo} > 0.3$).

The EC3 interaction approach has no constant curvature as those of the BS5950 and AISC/ECP approaches. That results in a good agreement between the interaction charts obtained from the EC3 approach and from the proposed design method. As can be concluded from Figs. 11 and 12, the interaction curve of the EC3 and proposed method are almost straight lines for short columns and their results are very close to those of the BS5950. For long columns, the curvature of the interaction curves obtained from EC3 and proposed method increase, but still very close to each other. This means that, the EC3 interaction approach is the most dynamic and the most accurate among the different approaches adopted by the design codes of practice.

6. Conclusions

From the current study, the following concluding remarks can be drawn:

1) Linear elastic interactive buckling in beam columns has been investigated using the finite element eigen-value analysis in comparison with the closed form solution available in literatures. Results of the finite element analysis were found to be in a very good agreement with the theoretical solution.
2) An analytical model based on Young's equation and similar to Perry formulation has been developed to predict the ultimate resistance of beam columns undergoing interactive buckling. This model takes into account the level of initial imperfection.

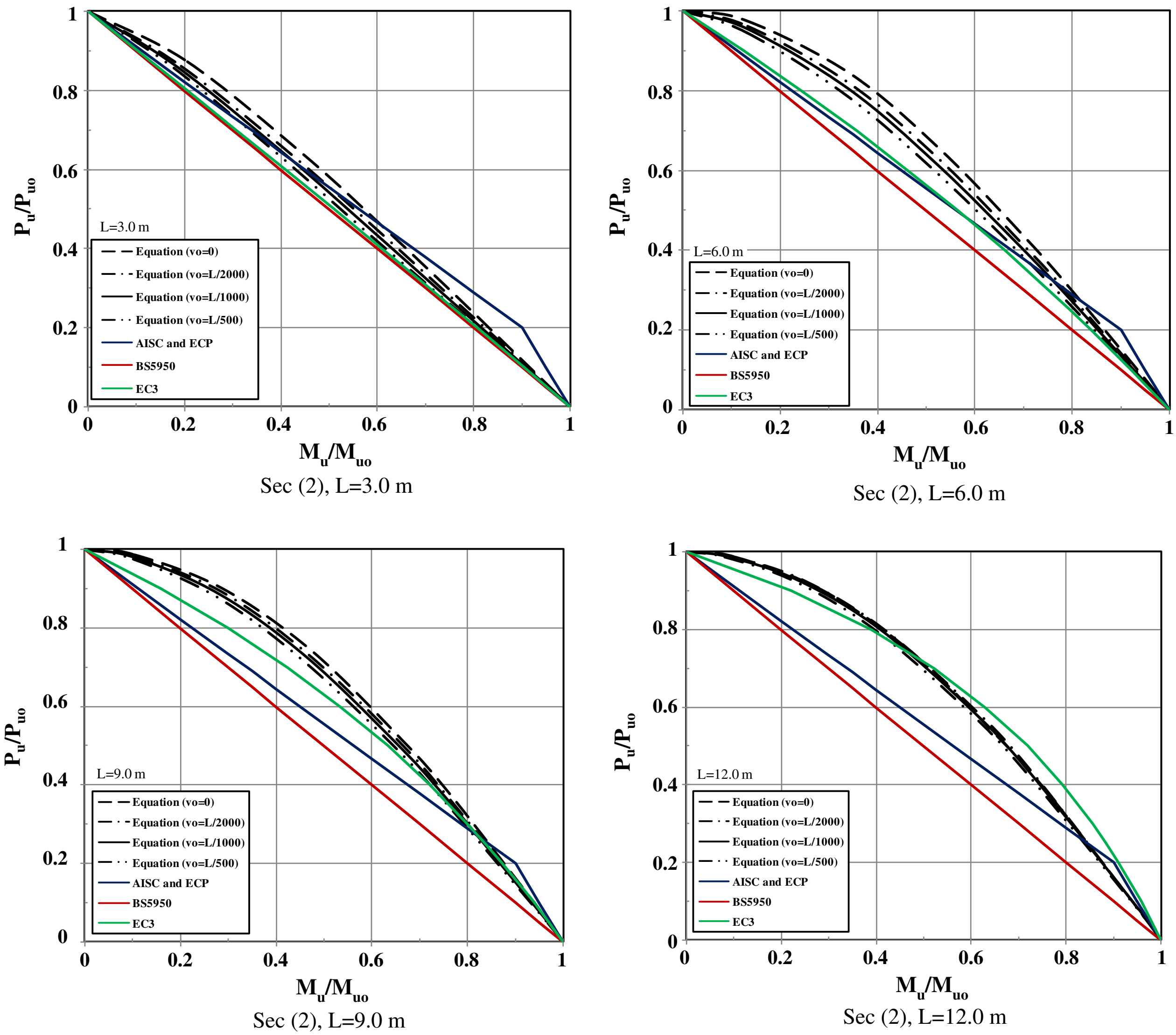

Fig. 12. Comparison between the proposed design method and the design codes methods for the second I-section, $b_f = 150$ mm, $t_f = 12$ mm, $d_w = 500$ mm, $t_w = 10$ mm, L = 3, 6, 9 and 12 m.

3) Finite element non-linear elasto-plastic analysis has been carried out using ANSYS 5.4 Program to validate the developed analytical model. It has been noticed that there is good agreement between the developed model and the finite element analysis for the investigated cases, for the ultimate resistance, force–displacement history and stress distribution at first yield, Figs. 7, 8, 9 and 10.
4) Interactive approaches adopted by the AISC, ECP, BS5950, and EC3 codes were investigated and compared with the finite element non-linear analysis as well as with the developed analytical model. The AISC-LRFD and ECP-LRFD use the same bilinear interactive approach. This approach gives conservative resistance for relatively long columns and for large normal force ($P_u/P_{uo}>0.35$), while for short columns and relatively small values of normal force ($P_u/P_{uo}<0.35$) the estimated strength is non-conservative. The BS5950 employs a straight line interactive approach which is always conservative compared to all other approaches. The EC3 interactive approach is the most flexible and most suitable approach that is capable to accurately predict the interactive resistance for all spans at all levels of eccentricity.
5) It has been shown that the developed analytical model accurately predicts the interactive strength compared to the finite element non-linear analysis and to the EC3 design approach. This model is still simple and applicable, as it implies the solution of a second order equation that can be achieved using a simple calculator. That means, the developed model is a rational but simple design tool.

References

[1] Allen HG, Bulson PS. Background to buckling. London: McGraw Hill Book Company LTD; 1989.
[2] American Institute of Steel Construction (AISC). Manual of Steel Construction. Chicago, Illinois, USA: Load and Resistance Factor Design (LRFD; March 2005.
[3] Aminmansour A. Steel beam-column design: new, fast, and practical approach. [Issue No 2]Practice periodical on structural design and construction, Volume: 9. American Society of Civil Engineers; 2004. p. 93–7. 1084–0680.
[4] ANSYS Release 5.4. Finite Element analysis Program; 1997.
[5] Attard MA. General and non-dimensional equation for lateral buckling. Thin Walled Struct 1990;9:417–35.
[6] Badawy Abu-sena AB. Ultimate resistance of beams undergoing lateral torsional buckling under uniform bending moment. 9th ICSGE Ain-Shams University, Cairo, Egypt, 10th to 12th December 2001; December 2001.
[7] British Standard (BS5950). Structural use of steel work in building. United Kingdom: Sheffield University; October 2002.
[8] Brockenbrough RL, Merritt FS. Structural Steel Designer's Handbook. Second Edition. New York: McGraw-Hill, Inc.; 1999.
[9] Champan JC, Buhagiar D. Application of Young's buckling equation to design against torsional buckling. Proc. of the Institution of Civil Eng., Structures and Buildings, No 10179, London, 1993; 1993. p. 359–69.

[10] ECP. Egyptian Code of Practice for Steel Constructions; Load and Resistance Factor Design (LRFD). First Edition. Cairo: Al-Ahram press; 2008.
[11] European Committee for Standardization (CEN), Euro code EC3. Design of Steel Structures, Part 1.1, General Rules and Rules for Buildings (ENV 1993-1-1); 1996.
[12] Geng-Shu T, Shao-Fan C. An interactive buckling theory for built-up beam-columns and its application to centrally compressed built-up members. J Constr Steel Res 1989;14(3):221–41.
[13] Gonçalves R, Camotim D. On the application of beam–column interaction formulae to steel members with arbitrary loading and support conditions. J Constr Steel Res 2004;60(3–5):433–50.
[14] Kanchanalai T. The design and behavior of beam-columns in un-braced steel frames. AISI Project No.189, Report No. 2, Civil Engineering, Structural Research Lab, University of Texas-Austin, October, 1977; October 1977.
[15] Trahair NS. Design strength of steel beam-columns. Structural Engineering Report No. 132, Department of Civil Engineering, University of Alberta, December, 1985; December 1985.
[16] Trahair NS, Bradford MA, Nethercot DA, Gardner L. The behavior and design of steel structures to EC3. Fourth Edition. New York, USA: Taylor and Francis; 2008.